Journal of Biomolecular NMR, **20:** 1–10, 2001.
KLUWER/ESCOM

Side chain mobility as monitored by CH-CH cross correlation: The example of cytochrome b_5

Lucia Banci, Ivano Bertini*, Isabella C. Felli, Parvana Hajieva & Maria Silvia Viezzoli
Magnetic Resonance Center (CERM), University of Florence, Via Luigi Sacconi 6, I-50019 Sesto Fiorentino (Florence), Italy

Received 9 November 2000; Accepted 22 January 2001

Key words: cross correlation, cytochrome, dynamics, side chain

Abstract

The mobility of βCH_2 moieties in oxidized and reduced cytochrome b_5 was studied by analyzing the ^{13}C relaxation of the J-split components, in terms of C-H dipole–C-H dipole cross correlation rates. A 2D ^{13}C-^{1}H experiment is proposed to measure these rates that provide the internal effective reorientation correlation time for each CH_2 moiety. It is found that higher mobility is present in the α helices forming the heme pocket. On the contrary, the β strands, which form the hydrophobic core of the molecule, have the lowest mobility. The general pattern is the same for the oxidized and reduced species, indicating that any oxidation-dependent property detected for backbone NH moieties does not affect the CH_2 mobility.

Abbreviations: cyt, cytochrome; Leu, leucine; Phe, phenylalanine; Trp, tryptophan; Tyr, tyrosine; His, histidine; Lys, lysine.

Introduction

It is now widely recognized that fluctuations of macromolecules around their average structure play a relevant role in determining their stability, their function and recognition of biological partners. NMR has made a real contribution to the study of local dynamics (Kay et al., 1989; Wagner, 1993; Palmer III, 1997; Kay, 1998). In particular, analysis of ^{15}N spin relaxation is currently used to determine local mobility of the backbone (Kay et al., 1989; Barbato et al., 1992; Peng and Wagner, 1992, 1994; Akke and Palmer III, 1996; Akke et al., 1998). The dynamics of side chains should be more pronounced and heterogeneous, since side chains are expected to have more degrees of freedom than the backbone. Studies of side chain dynamics, however, are still very few and are mainly based on deuterium relaxation studies (Nicholson et al., 1992; Buck et al., 1995; Yang et al., 1998; Mittermaier et al., 1999; Mulder et al., 2000). ^{13}C auto-relaxation rates are more difficult to exploit in terms of local dynamics due to complications introduced by C-C interactions in ^{13}C labeled proteins. A valuable alternative is provided by cross correlation rates. They arise from cross correlation between specific interactions and are also easier to identify and 'isolate' from other contributions to relaxation. Their favorable properties have given rise recently to a wealth of different applications, such as the TROSY approach, to larger macromolecules (Pervushin et al., 1997) and new methods to achieve structural and backbone dynamic information (Tjandra et al., 1996; Reif et al., 1997; Kroenke et al., 1998; Chiarparin et al., 1999, 2000; Felli et al., 1999; Pellecchia et al., 1999; Boisbouvier et al., 2000; Crowley et al., 2000). Some nice studies of longitudinal and rotating frame cross correlated relaxation involving methylene groups are available in the literature (Prestegard and Grant, 1978; Daragan and Mayo, 1993; Daragan et al., 1993; Ernst and Ernst, 1994). Recently, a straightforward approach to determination of transverse CH dipole–CH dipole cross correlated relaxation in the βCH_2 moiety has been proposed to

*To whom correspondence should be addressed. E-mail: bertini@cerm.unifi.it

obtain information on its reorientation (Yang et al., 1998). We propose here an alternative experiment, a variation of the HCCH experiment, to investigate CH dipole–CH dipole cross correlation involving βCH_2 groups. This approach was employed to study the side chain dynamics of rabbit microsomal cytochrome b_5 in both oxidation states involved in the physiological process.

Cytochrome b_5 is a membrane-bound heme protein involved in a variety of electron transfer reactions in which it shuttles electrons changing its oxidation state between Fe(II) and Fe(III) (Lederer, 1994). The hydrophilic domain, which retains activity, can be either isolated through tryptic cleavage (Ito and Sato, 1968; Spatz and Strittmatter, 1971) or expressed in *E. coli* (Von Bodman et al., 1986). Extensive structural and functional characterization is available from a variety of methods (Mathews, 1985; Lederer, 1994), making it an excellent candidate to address fundamental biological questions. NMR has been employed to explore the role of the polypeptide chain in modulating the properties of the metal cofactor and in determining its reactivity with redox partners. In particular, the solution structures and backbone dynamics of the rat isoenzyme in both oxidation states were determined (Banci et al., 1997c, 1998; Arnesano et al., 1998, 1999; Dangi et al., 1998a, b) to reveal any variations associated with electron transfer. Small and definite structural changes were indeed identified, in particular that of one of the two propionates (Arnesano et al., 1998, 1999). In addition, changes in backbone local mobility were observed as monitored by amide proton–deuterium exchange and rotating frame ^{15}N relaxation (Arnesano et al., 1998, 1999; Banci et al., 1998; Dangi et al., 1998). Structural and dynamic differences between the two oxidation states were also observed for other cytochromes (Banci et al., 1997a; Baxter and Fetrow, 1999; Fetrow and Baxter, 1999); these were proposed to be involved in protein–protein recognition with biological partners (Banci et al., 1997b; Arnesano et al., 1998; Sun et al., 1999).

We have here extended the characterization of local dynamics also to side chains, which should have more accessible degrees of freedom than the backbone and should display more heterogeneous behavior within the protein frame. Moreover, mobility of side chains on the surface of the protein may modulate the properties of the protein surface itself by changing, for example, the electrostatics through mobility of charged residues or by exposing more internal regions to the solvent. Experimental monitoring of the motions of side chains is important to an understanding of how the protein surface adjusts to interact with biological partners.

Materials and methods

Sample preparation

Cytochrome b_5 was isolated from *Escherichia coli* strain TOPP2, containing the plasmid pKK223-3 carrying the gene coding for the 98-amino acid polypeptide corresponding to the soluble part of microsomal rabbit cytochrome b_5 (generously provided by A.W. Steggles, Northeastern Ohio Universities College of Medicine, OH, U.S.A.). The procedure has been reported previously for rat cytochrome b_5 (Von Bodman et al., 1986). To prepare the ^{15}N-^{13}C labeled samples, *E. coli* cells were transformed with the plasmid and plated on to Luria–Bertani agarose containing 100 $\mu g \cdot ml^{-1}$ ampicillin. A 10 ml volume of Luria–Bertani medium containing 100 $\mu g \cdot ml^{-1}$ ampicillin was inoculated from a single colony, and cultured overnight at 37 °C with shaking. The inoculum was then transferred to a 2 l flask containing 1 l minimal medium with 50 $\mu g \cdot ml^{-1}$ ampicillin. The culture was grown with shaking at 37 °C up to an A_{600} of about 0.8, and then induced with 0.5 mM isopropyl β-D-thiogalactopiranoside. The culture was harvested by centrifugation after 15 h from induction. The protein was extracted from the *E. coli* cells as described previously (Von Bodman et al., 1986). The minimal medium used for cultures consisted of M9 salts supplemented with $MgSO_4$, trace metal and vitamin solutions. The nitrogen source was $(^{15}NH_4)_2SO_4$ (1.2 $g \cdot l^{-1}$), and the carbon source was glycerol (1 $g \cdot l^{-1}$). About 10 mg of the purified protein was exchanged through ultrafiltration with 50 mM potassium phosphate buffer in D_2O at pH 7.5. The sample was maintained in the oxidized state under oxygen while sodium dithionite, under anaerobic conditions, was added in slight excess to obtain the fully reduced form. In each case, the final protein concentration was about 1.5 mM.

NMR experiments

Experiments were performed on a Bruker Avance 800 MHz NMR spectrometer equipped with a ^{1}H,^{13}C,^{15}N TXI probe with z pulsed field gradients. ^{1}H-^{13}C 2D correlation experiments were obtained with the pulse sequence reported in Figure 1. They were repeated with the same experimental parameters

for the oxidized and reduced protein samples. All data were recorded as complex matrices of 2048×165 data points and spectral widths of 15.01 ppm and 40.2 ppm in the direct ^{1}H dimension and indirect ^{13}C dimension, respectively. Quadrature detection in ω_1 was achieved by incrementing the phase of the ^{13}C 90° pulse before the evolution time in the TPPI fashion. A recycle delay of 1.1 s was employed. For each increment, 160 scans were used for a total acquisition time of about 16 h. Experiments were acquired with T = 7.1, 21.4, 35.7 ms. The Δ delay was set to 3.4 ms ($1/2J_{CH}$), the delay Δ' to 1.7 ms ($1/4J_{CH}$) and T′ to 14.2 ms ($1/2J_{CC}$). An additional experiment optimized for detection of AMX amino acids with T = 14.2 ms ($1/2J_{CC}$), 110 complex points in the ^{13}C dimension was acquired. Composite pulse decoupling was applied during acquisition with an RF field strength of 2.5 kHz. Data were processed and analyzed with the standard Bruker software.

Methodological aspects

Auto relaxation rates involving carbon spins may be very difficult to interpret in terms of local dynamics due to the many carbon–carbon interactions that complicate the process. Relaxation rates arising from cross correlations between different interactions can offer alternative approaches to study local dynamics (Prestegard and Grant, 1978; Daragan and Mayo, 1993; Daragan et al., 1993; Ernst and Ernst, 1994; Yang et al., 1998). We focus here on the CH dipole–CH dipole cross correlation rate $\Gamma_{CH1,CH2}$ in βCH_2 systems. This arises from the interference between the two carbon–proton dipolar interactions involving the carbon spin and the two geminal protons. The $\Gamma_{CH1,CH2}$ rate is given by (Yang et al., 1998):

$$\Gamma_{CH1,CH2} = \frac{\gamma_H^2 \gamma_C^2 \hbar^2}{r_{CH}^6}\left[J_{CH1,CH2}(0) + \frac{3}{4} J_{CH1,CH2}(\omega_C) \right] \quad (1)$$

where γ_H, γ_C are the gyromagnetic ratios of proton and carbon and r_{CH} is the carbon–proton distance. The $J_{CH1,CH2}$ (ω) terms are given by (Yang et al., 1998):

$$J_{CH1,CH2}(\omega) = \frac{2}{5}\left[S^2_{CH1,CH2} \frac{\tau_c}{1+\omega^2\tau_c^2} + \left(P_2\left(\cos\theta_{CH1,CH2}\right) - S^2_{CH1,CH2} \right) \frac{\tau}{1+\omega^2\tau^2} \right] \quad (2)$$

where $\tau^{-1} = \tau_c^{-1} + \tau_e^{-1}$, τ_c and τ_e are the overall rotational and internal correlation times, respectively, and $S^2_{CH1,CH2}$ is the cross correlation order parameter and $P_2(\cos\theta_{CH1,CH2}) = (3\cos\theta^2_{CH1,CH2}\theta 1)/2$ where $\theta_{CH1,CH2}$ is the angle between the two CH bond vectors.

Since the CH_2 group can be approximated to a system with fixed geometry, the contribution to the rate arising from the relative orientations of the two carbon–proton dipolar interactions is a known constant. Therefore, differences in the $\Gamma_{CH1,CH2}$ rate for different residues within a given protein can be interpreted in terms of differences in $J_{CH1,CH2}(\omega)$. Furthermore, assuming for the moment isotropic reorientation of the molecule, differences in $J_{CH1,CH2}(\omega)$ can be interpreted in terms of local motions.

The 2D ^{1}H-^{13}C NMR experiment proposed here measures the CH dipole–CH dipole cross correlation rate through an HCCH-type approach and adopts a J-resolved method as in the one proposed by Kay and co-workers (Yang et al., 1998). Another sequence available for obtaining CH dipole–CH dipole cross correlation in H_1-C_1-C_2-H_2 groups (Felli et al., 1999) is not as appropriate and selective for the CH_2 groups. The experiment proposed here involves only ^{1}H and ^{13}C nuclei, and does not require evolution of ^{15}N nuclei. Therefore it can be applied to protein samples labeled only in ^{13}C and it can be advantageous when NH protons are not detectable, such as at high pH. The pulse sequence is shown in Figure 1. Single quantum coherence is transferred from proton (for example, $H^{\beta 1}$) to the directly attached carbon (C^{β}) in an INEPT fashion. C^{β}_x is selected at time *a* and is followed by a constant time evolution period. The constant time (T) is set to $(2n+1)/4J_{CC}$ in order to obtain $2C^{\beta}_y C^{\alpha}_z$ at time *b*. The couplings with carbonyls are refocused by the two selective 180° pulses on carbonyls. The subsequent ^{13}C 90° pulse converts $2C^{\beta}_y C^{\alpha}_z$ into $2C^{\beta}_z C^{\alpha}_y$ (time *c*). The latter coherence then evolves during T′ according to J_{CC} and during Δ according to J_{CH}. At time *d* the component $2H^{\alpha}_z C^{\alpha}_y$ is converted into detectable proton single quantum coherence. The latter leads to cross peaks at (ω^{α}_H, ω^{β}_C) for which one-bond CH couplings of C^{β} are resolved in the indirect dimension.

During the constant time period, each component of the CH multiplet relaxes, to a good approximation, with the following rates (Kay and Bull, 1992):

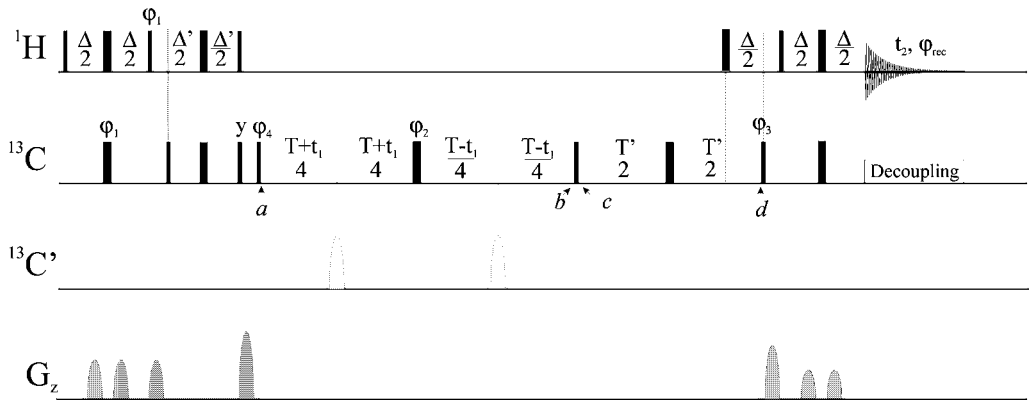

Figure 1. Pulse sequence of the 2D ^{1}H-^{13}C experiment to measure $\Gamma_{CH1,CH2}$. Narrow and thick bars represent 90° and 180° pulses. The default phase for pulses is x. $\Delta = 3.4$ ms and $\Delta' = 1.7$ ms, T = 7.1, 21.4 and 35.7 ms, T′ = 14.2 ms. ^{13}C-decoupling was applied during acquisition with $\gamma B_1/2\pi = 2.5$ kHz. The two shaped pulses are 250 μs with a G3 shape (Emsley and Bodenhausen, 1990) and a phase modulation of 125 ppm with the ^{13}C carrier placed at 40 ppm. Gradients were all 1 ms long with a sine shape and their strengths were the following: 15, 15, 17.5, 37.5, 24, 11.5, 11.5 G/cm. The phase cycle employed was: φ_1 = y, −y; φ_2 = 8(y), 8(−x), 8(−y), 8(x); φ_3 = 2(x), 2(−x); φ_4 = 4(y), 4(−y); φ_{rec} = x, 2(−x), x, −x, 2(x), −x, −x, 2(x), −x, x, 2(−x), x.

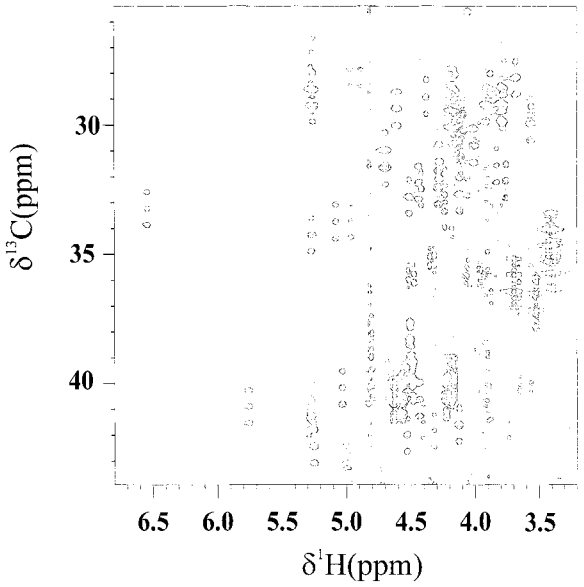

Figure 2. 800 MHz ^{1}H-^{13}C 2D spectrum of reduced rabbit cytochrome b_5 obtained with the experiment shown in Figure 1 (T = 21.4 ms). The region containing ($\omega_{H\alpha}$, $\omega_{C\beta}$) connectivities is shown.

$$\begin{aligned}\Gamma_{\alpha\alpha} &= \Gamma^a + \Gamma_{CH1,CH2} + \Gamma_{C,CH1} + \Gamma_{C,CH2} + W_2\\ \Gamma_{\alpha\beta+\beta\alpha} &= \Gamma^a - \Gamma_{CH1,CH2}\\ \Gamma_{\beta\beta} &= \Gamma^a + \Gamma_{CH1,CH2} - \Gamma_{C,CH1} - \Gamma_{C,CH2} + W_2\end{aligned} \quad (3)$$

where Γ^a is the autorelaxation rate, $\Gamma_{CH1,CH2}$ is the CH dipole–CH dipole cross correlation rate, $\Gamma_{C,CH1}\Gamma_{C,CH2}$ are the (carbon) CSA–(carbon–proton) dipole cross correlation rates and W_2 is the transition probability between the αα and ββ proton states. The latter can safely be neglected in the slow motion limit (Solomon, 1955). The $\Gamma_{\alpha\beta+\beta\alpha}$ does not contain $\Gamma_{C,CH1}$ and $\Gamma_{C,CH2}$ because the two terms cancel each other and, since they are small, to a good approximation they can be neglected (Prestegard and Grant, 1978; Yang et al., 1998).

The intensity of each multiplet component is then given by:

$$\begin{aligned}I_{\alpha\alpha}(\mathrm{T}) &= I(0)\exp(-\Gamma_{\alpha\alpha}T)\\ I_{\beta\beta}(\mathrm{T}) &= I(0)\exp(-\Gamma_{\beta\beta}T)\\ I_{\alpha\beta+\beta\alpha}(\mathrm{T}) &= 2I(0)\exp(-\Gamma_{\alpha\beta+\beta\alpha}T)\end{aligned} \quad (4)$$

The rate $\Gamma_{CH1,CH2}$ can be determined by combining Equations 3 and 4 (Yang et al., 1998):

$$\Gamma_{CH1,CH2} = -\left[1/(4T)\right]\ln\left[\left(4I_{\alpha\alpha}(T)I_{\beta\beta}(T)\right)/I^2_{\alpha\beta+\beta\alpha}(T)\right] \quad (5)$$

where $I_{\alpha\alpha}$, $I_{\alpha\beta+\beta\alpha}$, $I_{\beta\beta}$ are the intensities of the three resolved components of the ^{13}C multiplets.

Results and discussion

Reduced cytochrome b_5

The experiment shown in Figure 1 was applied to reduced cytochrome b_5. Out of the 70 residues in cytochrome b_5 containing a βCH_2 group, 37 provided resonances sufficiently well resolved to allow safe integration and intensity determination to estimate the

rates $\Gamma_{CH1,CH2}$. As an example, Figure 2 shows the Hα-Cβ region of the spectrum. In the indirect ^{13}C dimension cross peaks show the resolved C-H one-bond couplings which, for CH_2 moieties, yield a triplet. In the absence of cross correlation, the multiplet components along the ^{13}C dimension should display an intensity pattern of 1:2:1 (this has been verified by changing the constant time evolution into real time evolution). On the other hand, if the different multiplet components relax at different rates, their relative intensities will deviate from the 1:2:1 pattern.

The intensity deviations will increase as both the differential relaxation and the evolution time (T) increase (see Equation 4). Experiments were repeated for different values of T to ensure that the observed deviations from the 1:2:1 pattern were indeed increasing with the evolution time during which cross correlation rates on the multiplet components develop. Figure 3 reports representative traces along the ^{13}C dimensions of two different ($\omega_{H\alpha}$, $\omega_{C\beta}$) correlations corresponding to Glu 43 and Tyr 7 in reduced cytochrome b_5. The two residues were chosen because they exhibit a very different behavior. For residue 43 the deviation of the multiplet from a 1:2:1 intensity pattern is rather small (also at longer values of T), indicating that the cross correlation rate is close to zero. As the cross correlation is modulated by the resulting correlation time for the overall tumbling and local motions, the presence of fast internal motions (i.e. faster than the overall tumbling) reduces the cross correlation term to relaxation. Therefore the behavior of the multiplet of Glu 43 indicates the existence of fast internal motions. On the other hand, deviations from the 1:2:1 intensity pattern for Tyr 7 are quite pronounced and increase with increasing T. This is due to a much larger absolute value of $\Gamma_{CH1,CH2}$ as a consequence of a larger correlation time and indicates that this CH_2 group is characterized by a lower mobility.

Rates were estimated by measuring the intensities of the three multiplet components and using Equation 5. They are plotted against residue number in Figure 4 (filled squares). The largest measured rates (in absolute value) provide a correlation time of about 7.5 ± 1 ns using $\theta_{CH1,CH2} = 109.5°$ and $r_{CH} = 1.09$ Å. Since the measurements are performed in D_2O (viscosity 30% higher than H_2O), the correlation time is consistent with the values obtained from model free analysis of ^{15}N relaxation rate measurements on the rat isoenzyme (5.6 and 5.9 ns for the two isoforms; Arnesano et al., 2000). Motions with time scales that are shorter than the overall rotational correlation time contribute to a shorter effective correlation time and cause a decrease in $\Gamma_{CH1,CH2}$. Independent of the motional model (Daragan and Mayo, 1997), comparison of $\Gamma_{CH1,CH2}$ values for different residues of the protein can be used to produce a picture of differential local mobility in the protein frame.

The elements of secondary structure present in the protein (Arnesano et al., 1998; Banci et al., 2000) are shown in Figure 4 as shaded areas (dark ones represent α helices, light ones β strands). The majority of the more flexible residues are located in α helices while most of the less flexible ones are found in β strands. This observation indicates that the heme pocket is formed by more flexible helices, in particular helices α_2 and α_3, supported by tightly packed, less flexible β strands. Interestingly, most of the more flexible residues are charged, indicated with arrows on top of Figure 4. Hydrophobic residues are generally less flexible, in particular aromatic ones with large steric hindrance such as Tyr 6, 7, 30, Phe 35, Trp 22. Again, this finding agrees with the picture that most charged residues are solvent exposed, whereas hydrophobic residues tend to pack more tightly in the interior of the protein. The results are mapped in the protein frame in Figure 5A. The different mobility is represented as shades of red-to-green with red being more rigid and green more flexible. The β sheet, which can be seen as a vertical patch of 'red' residues at the back of the heme, is characterized by more rigid residues, including Lys 28 which is charged and more peripheral, being close to the surface. In helix α_2, charged residues whose side chains point towards the solvent (Lys 34, Glu 37, Glu 38) are very mobile while hydrophobic ones (Phe 35, Leu 36), whose side chains point towards the protein interior, are less flexible (Figure 6). The aromatic ring of Phe 35 points straight towards the heme and has been shown to be important in stabilizing the heme pocket through point mutations in which Phe 35 was converted to Tyr, Leu and His (Yao et al., 1997). The very low mobility identified here for the βCH_2 group of Phe 35 is consistent with the role of this residue in stabilizing the heme pocket. Helix α_2 is separated from the following one by histidine 39 which, together with His 63, coordinates the iron ion. As expected, these histidines are not flexible, particularly His 39. This observation is further support for their important role in stabilizing the heme–protein interaction (Figure 6). Indeed, mutation of His 63 into alanine renders the heme pocket so unstable that the heme is not incorporated (Von Bodman et al., 1986). His 63 is found to be relatively more mobile than His

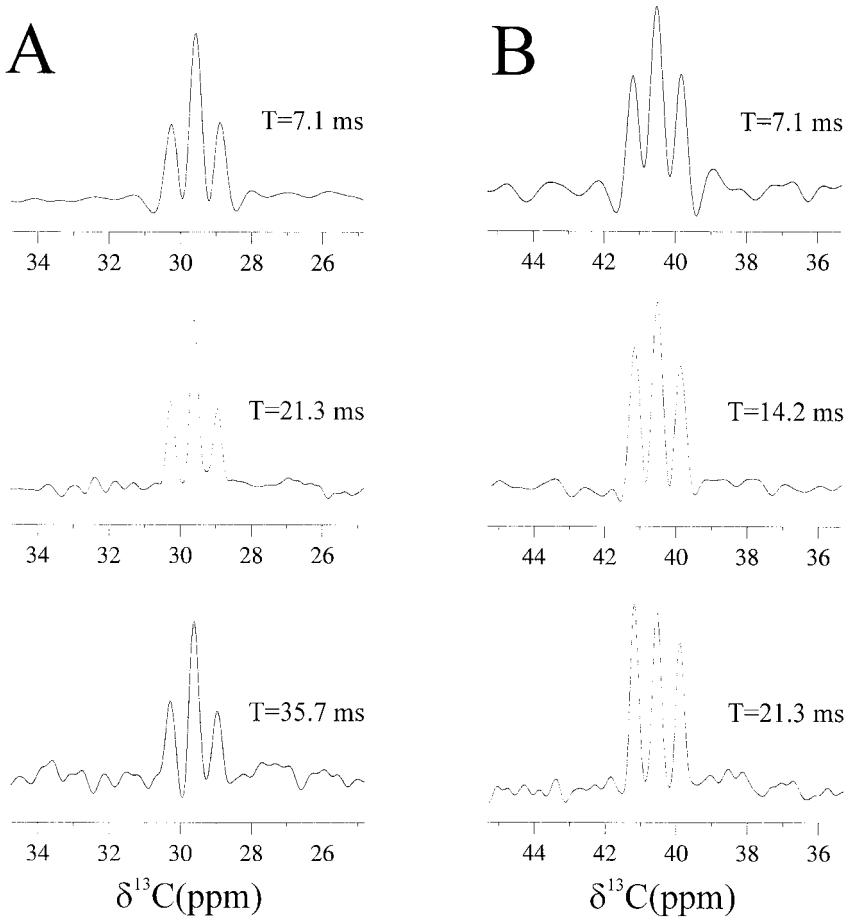

Figure 3. Representative traces taken from 800 MHz 2D ^{1}H-^{13}C spectra acquired with the sequence reported in Figure 1 on reduced cytochrome b_5 along the ^{13}C dimension for Glu 43 (A) and Tyr 7 (B). The traces are taken from spectra that differ in the time T (shown in the figure). It can be noted that variations due to the cross correlation rate $\Gamma_{CH1,CH2}$, as the relaxation time T increases, are very small for Glu 43 (A) and much more pronounced for Tyr 7 (B).

39, in agreement with studies of the apo form of cytochrome b_5 in which residues near His 63 are found to be more disordered (Falzone et al., 1996; Bhattacharya et al., 1999). Continuing along the primary sequence, helix α_3 is rich in charged residues that are proposed to interact with cytochrome *c* and which may be relevant for interaction with other positively charged proteins (Mauk et al., 1982; Eley and Moore, 1983; Wendoloski et al., 1987; Rodgers et al., 1988; Burch et al., 1990; Sun et al., 1996). All of the residues identified belonging to this helix are very flexible. Indirect evidence suggests that cytochrome b_5 and redox partners do not interact via rigid complementary surfaces, but via induced fits of adaptable modules that still retain a certain degree of flexibility after complex formation (Salemme, 1976; Burch et al., 1990; Guiles et al., 1996; Arnesano et al., 1998). Identification of elevated local side chain mobility in helix α_3 proves experimentally that the protein surface, in addition to providing electrostatic interactions to attract redox partners, also has easily accessible degrees of freedom to adapt to the redox partner. The remaining two helices forming the heme binding pocket are still characterized by relatively high local mobility, even if this behavior is less pronounced with respect to the two previous ones.

In summary, the differences in local mobility observed for the various parts of the protein clearly show the structural role of the β sheet, which constitutes the hydrophobic core of the molecule. In addition, the two coordinating histidines confer rigidity to the molecule and stabilize interactions in the hydrophobic heme pocket. A more flexible region contains the helices and is constituted mainly of hydrophilic residues but includes some structurally important hydrophobic

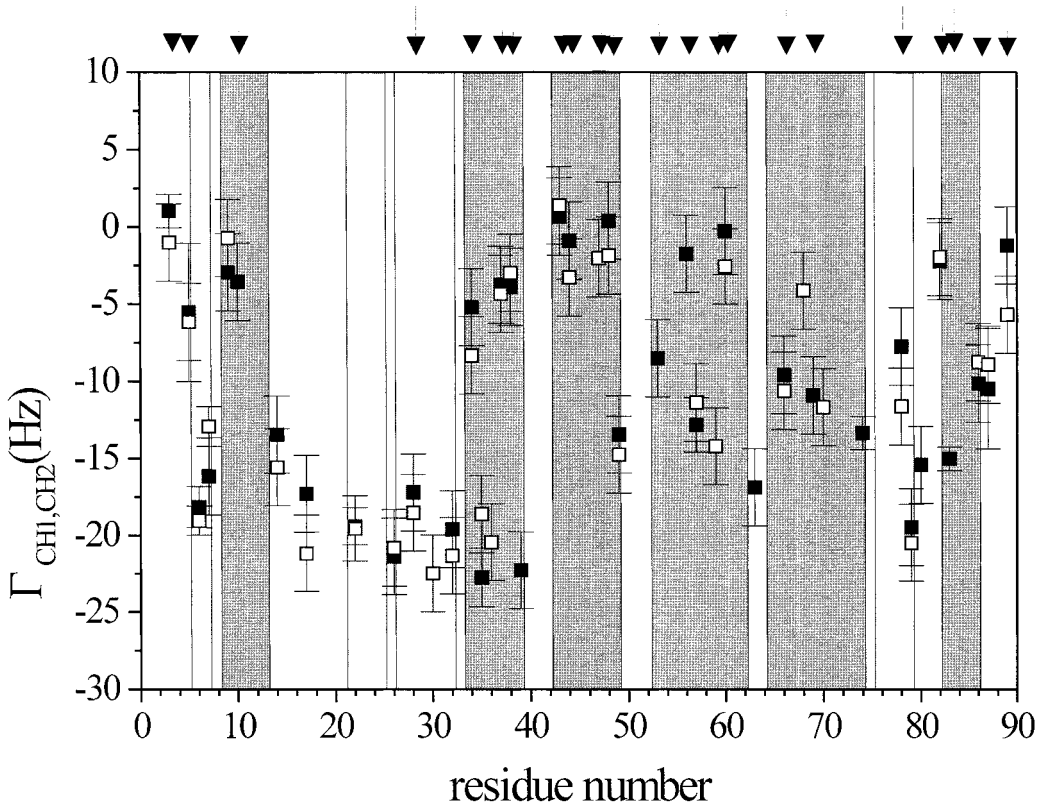

Figure 4. The rates $\Gamma_{CH1,CH2}$ are plotted against the residue number for the reduced (filled squares) and oxidized (open squares) forms of cytochrome b_5. The shaded areas represent the secondary structural elements identified in rabbit cytochrome b_5 (Banci et al., 2000): dark ones are helices α_1 (8–13), α_2 (33–39), α_3 (42–49), α_4 (52–62), α_5 (64–74), α_6 (82–84) and light ones are β strands β_1 (5–7), β_2 (21–25), β_3 (26–32), β_4 (75–79). The arrows at the top indicate charged residues.

residues, such as Phe 35. The regions characterized by high mobility are involved in molecular recognition of biological partners in the electron transfer process. This is particularly interesting, as local mobility of side chains reflects modulation of the protein surface.

Oxidized cytochrome b_5

The experiments were repeated on oxidized cytochrome b_5. In this case, 34 residues provided resonances sufficiently resolved to allow safe integration and intensity determination for estimation of the rates $\Gamma_{CH1,CH2}$. The results are plotted against residue number in Figure 4 (empty squares). Within experimental error, no marked differences in local mobility are observed between the two oxidation states. However, the striking differences in mobility observed over the protein frame are retained in the oxidized form. The results are mapped in the protein frame in Figure 5B. Although the sampling is not identical for the two redox states, the overall behavior is similar.

Comparison with backbone dynamics

Studies of backbone dynamics are available for the rat isoenzyme in the two oxidation states (Kelly et al., 1997; Banci et al., 1998; Dangi et al., 1998a, b; Arnesano et al., 1999). As the rat isoenzyme differs from the rabbit isoenzyme only in 6 residues, a meaningful comparison of the data can be attempted. The studies of backbone local mobility through NH exchange and through rotating frame ^{15}N relaxation experiments (μs–ms time scale) performed on cytochrome b_5 revealed that local mobility depends markedly on the oxidation state of the iron ion (Arnesano et al., 1998, 1999; Banci et al., 1998; Dangi et al., 1998). The oxidized form is more flexible than the reduced form (Arnesano et al., 1998, 1999; Banci et al., 1998). Similar behavior was also found for cytochrome *c* (Baistrocchi et al., 1996; Banci et al., 1997a, b, 1999; Baxter and Fetrow, 1999; Fetrow and Baxter, 1999). However, on a faster time scale (ns–ps), the differences in local mobility, as resulting from model

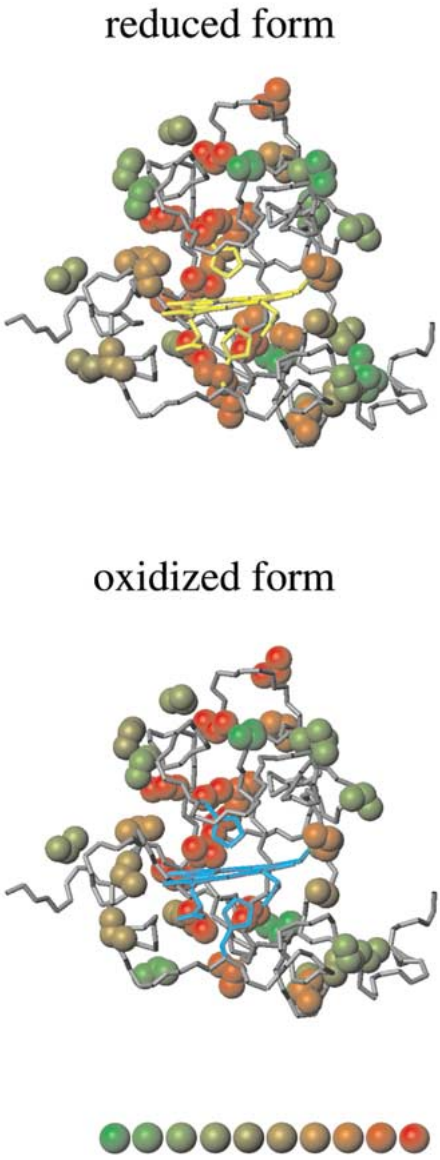

Figure 5. Mapping of the side chain $\Gamma_{CH1,CH2}$ rates on the structure of oxidized rabbit cytochrome b_5 as obtained in solution through NMR (Banci et al., 2000). Data are shown both for the reduced (top) and for the oxidized form (bottom). Experimental data are available only for βCH_2 pairs shown as spheres. Each sphere belonging to a CH_2 group is colored according to the observed $\Gamma_{CH1,CH2}$. The color coding used for $\Gamma_{CH1,CH2}$, represented at the bottom of the figure, is the following: $\Gamma_{CH1,CH2} < -20$ Hz corresponds to red and then each different shade corresponds to an increase of 2 Hz.

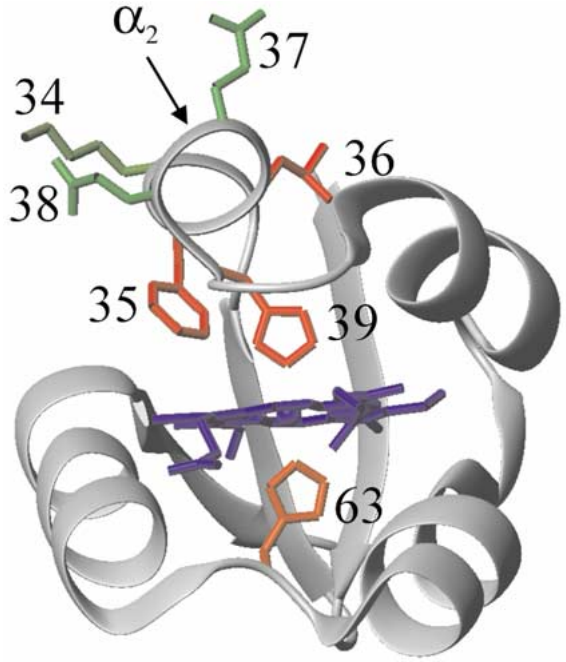

Figure 6. Ribbon representation of heme pocket as defined by residues 20–80 (Banci et al., 2000). The different dynamic behavior of side chains in helix α_2 and of the two histidines is shown. The side chains are color coded as in Figure 5. The ribbon is shown in grey and the heme is displayed in blue.

free analysis, between the two oxidation states are attenuated significantly for both cytochrome *c* and cytochrome b_5 (Dangi et al., 1998; Fetrow and Baxter, 1999). The cross correlation rate $\Gamma_{CH1,CH2}$ measured to monitor side chain mobility is sensitive to motions faster than the rotational correlation time (Yang et al., 1998) and no marked differences in side chain local mobility were identified between the two oxidation states (within experimental error). Differences could be within the experimental error, but in this case they would be rather small. This is consistent with attenuated differences in backbone local mobility between the two oxidation states on fast time scales. Within the protein frame a similar trend for backbone and side chain local mobility is observed for the β strands between residues 20 and 30 (which remain rigid in both states) and for residues 37 and 38 (which are instead very flexible). The rest of the data do not show obvious correlations. This is not surprising since, on one hand, fluctuations of the NH group that propagate through the backbone to the βCH_2 group can be attenuated, and on the other, βCH_2 groups have many more degrees of freedom than the backbone.

Concluding, side chain dynamics monitored through determination of the CH dipole–CH dipole cross correlation rate $\Gamma_{CH1,CH2}$ clearly suggests that differences in local mobility can have a functional role: the rigid β strand supports the heme pocket, while the more flexible helices constituting the protein surface form an adaptable module which can allow the protein to interact with redox partners.

Acknowledgements

Thanks are expressed to Ad Bax for useful discussions. Financial support of the EU through contracts HPRN-CT-2000-00092 and HPRI-CT-1999-00009 is gratefully acknowledged. This work has also been partly supported by MURST ex 40% 1999 (Italy).

References

Akke, M., Liu, J., Cavanagh, J., Erickson, H.P. and Palmer III, A.G. (1998) *Nat. Struct. Biol.*, **5**, 55–59.

Akke, M. and Palmer III, A.G. (1996) *J. Am. Chem. Soc.*, **118**, 911–912.

Arnesano, F., Banci, L., Bertini, I. and Felli, I.C. (1998) *Biochemistry*, **37**, 173–184.

Arnesano, F., Banci, L., Bertini, I., Felli, I.C. and Koulougliotis, D. (1999) *Eur. J. Biochem.*, **260**, 347–354.

Arnesano, F., Banci, L., Bertini, I., Koulougliotis, D. and Monti, A. (2000) *Biochemistry*, **39**, 7117–7130.

Baistrocchi, P., Banci, L., Bertini, I., Turano, P., Bren, K.L. and Gray, H.B. (1996) *Biochemistry*, **35**, 13788–13796.

Banci, L., Bertini, I., Bren, K.L., Gray, H.B., Sompornpisut, P. and Turano, P. (1997a) *Biochemistry*, **36**, 8992–9001.

Banci, L., Bertini, I., Cavazza, C., Felli, I.C. and Koulougliotis, D. (1998) *Biochemistry*, **37**, 12320–12330.

Banci, L., Bertini, I., Ferroni, F. and Rosato, A. (1997c) *Eur. J. Biochem.*, **249**, 270–279.

Banci, L., Bertini, I., Gray, H.B., Luchinat, C., Reddig, T., Rosato, A. and Turano, P. (1997b) *Biochemistry*, **36**, 9867–9877.

Banci, L., Bertini, I., Huber, J.G., Spyroulias, G.A. and Turano, P. (1999) *J. Biol. Inorg. Chem.*, **4**, 21–31.

Banci, L., Bertini, I., Rosato, A. and Scacchieri, S. (2000) *Eur. J. Biochem.*, **267**, 755–766.

Barbato, G., Ikura, M., Kay, L.E., Pastor, R.W. and Bax, A. (1992) *Biochemistry*, **31**, 5269–5278.

Baxter, S.M. and Fetrow, J.S. (1999) *Biochemistry*, **38**, 4493–4503.

Bhattacharya, S., Falzone, C.J. and Lecomte, J.T.J. (1999) *Biochemistry*, **38**, 2577–2589.

Boisbouvier, J., Brutscher, B., Pardi, A., Marion, D. and Simorre, J.P. (2000) *J. Am. Chem. Soc.*, **122**, 6779–6780.

Buck, M., Boyd, J., Redfield, C., MacKenzie, D.A., Jeenes, D.J., Archer, D.B. and Dobson, C.M. (1995) *Biochemistry*, **34**, 4041–4055.

Burch, A.M., Rigby, S.E.J., Funk, W.D., MacGillivray, R.T.A., Mauk, M.R., Mauk, A.G. and Moore, G.R. (1990) *Science*, **247**, 831–833.

Chiarparin, E., Pelupessy, P., Ghose, R. and Bodenhausen, G. (1999) *J. Am. Chem. Soc.*, **121**, 6876–6883.

Chiarparin, E., Pelupessy, P., Ghose, R. and Bodenhausen, G. (2000) *J. Am. Chem. Soc.*, **122**, 1758–1761.

Crowley, P., Ubbink, M. and Otting, G. (2000) *J. Am. Chem. Soc.*, **122**, 2968–2969.

Dangi, B., Blankman, J., Miller, C.J., Volkman, B.F. and Guiles, R.D. (1998a) *J. Phys. Chem. B*, **102**, 8201–8208.

Dangi, B., Sarma, S., Yan, C., Banville, D.L. and Guiles, R.D. (1998b) *Biochemistry*, **37**, 8289–8302.

Daragan, V., Kloczewiak, M.A. and Mayo, K.H. (1993) *Biochemistry*, **32**, 10580–10590.

Daragan, V. and Mayo, K.H. (1993) *Biochemistry*, **32**, 11488–11499.

Daragan, V. and Mayo, K.H. (1997) *Progr. NMR Spectrosc.*, **31**, 63–105.

Eley, C.G.S. and Moore, G.R. (1983) *J. Biochem.*, **215**, 11–21.

Emsley, L. and Bodenhausen, G. (1990) *Chem. Phys. Lett.*, **165**, 469–476.

Ernst, M. and Ernst, R.R. (1994) *J. Magn. Reson.*, **A110**, 202–213.

Falzone, C.J., Mayer, M.R., Whiteman, E.L., Moore, C.D. and Lecomte, J.T.J. (1996) *Biochemistry*, **35**, 6519–6526.

Felli, I.C., Richter, C., Griesinger, C. and Schwalbe, H. (1999) *J. Am. Chem. Soc.*, **121**, 1956–1957.

Fetrow, J.S. and Baxter, S.M. (1999) *Biochemistry*, **38**, 4480–4492.

Guiles, R.D., Sarma, S., DiGate, R.J., Banville, D., Basus, V.J., Kuntz, I.D. and Waskell, L. (1996) *Nat. Struct. Biol.*, **3**, 333–339.

Ito, A. and Sato, R. (1968) *J. Biol. Chem.*, **243**, 4922–4923.

Kay, L.E. (1998) *Nat. Struct. Biol.*, **5**, 513–517.

Kay, L.E. and Bull, T.E. (1992) *J. Magn. Reson.*, **99**, 615–622.

Kay, L.E., Torchia, D.A. and Bax, A. (1989) *Biochemistry*, **28**, 8972–8979.

Kelly, G.P., Muskett, F.W. and Whitford, D. (1997) *Eur. J. Biochem.*, **245**, 349–354.

Kroenke, C.D., Loria, J.P., Lee, L.K., Rance, M. and Palmer III, A.G. (1998) *J. Am. Chem. Soc.*, **120**, 7905–7915.

Lederer, F. (1994) *Biochimie*, **76**, 674–692.

Mathews, F.S. (1985) *Progr. Biophys. Mol. Biol.*, **45**, 1–56.

Mauk, M.R., Reid, L.S. and Mauk, A.G. (1982) *Biochemistry*, **21**, 1843–1846.

Mittermaier, A., Varani, L., Muhandiram, D.R., Kay, L.E. and Varani, G. (1999) *J. Mol. Biol.*, **294**, 967–979.

Mulder, F.A., Hon, B., Muhandiram, D.R., Dahlquist, F.W. and Kay, L.E. (2000) *Biochemistry*, **39**, 12614–12622.

Nicholson, L.K., Kay, L.E., Baldisseri, D.M., Arango, J., Young, P.E, Bax, A. and Torchia, D.A. (1992) *Biochemistry*, **31**, 5253–5263.

Palmer III, A.G. (1997) *Curr. Opin. Struct. Biol.*, **7**, 732–737.

Pellecchia, M., Pang, Y., Wang, L., Kurochkin, A.V., Kumar, A. and Zuiderweg, E.R.P. (1999) *J. Am. Chem. Soc.*, **121**, 9165–9170.

Peng, J.W. and Wagner, G. (1992) *J. Magn. Reson.*, **98**, 308–332.

Peng, J.W. and Wagner, G. (1994) *Methods Enzymol.*, **239**, 563–596.

Pervushin, K., Riek, R., Wider, G. and Wüthrich, K. (1997) *Proc. Natl. Acad. Sci. USA*, **94**, 12366–12371.

Prestegard, J.H. and Grant, D.M. (1978) *J. Am. Chem. Soc.*, **100**, 4664–4668.

Reif, B., Hennig, M. and Griesinger, C. (1997) *Science*, **276**, 1230–1233.

Rodgers, K.K., Pochapsky, T.C. and Sligar, S.G. (1988) *Science*, **240**, 1657–1659.

Salemme, F.R. (1976) *J. Mol. Biol.*, **102**, 563–568.

Solomon, I. (1955) *Phys. Rev.*, **99**, 559–565.

Spatz, L. and Strittmatter, P. (1971) *Proc. Natl. Acad. Sci. USA*, **68**, 1042–1046.
Sun, Y.L., Wang, Y.H., Yan, M.M., Sun, B.Y., Xie, Y., Huang, Z.X., Jiang, S.K. and Wu, H.M. (1999) *J. Mol. Biol.*, **285**, 347–359.
Sun, Y.L., Xie, Y., Wang, Y.H., Xiao, G.T. and Huang, Z.X. (1996) *Protein Eng.*, **9**, 555–558.
Tjandra, N., Szabo, A. and Bax, A. (1996) *J. Am. Chem. Soc.*, **118**, 6886–6891.
Von Bodman, S.B., Schulder, M.A., Jollie, D.R. and Sligar, S.G. (1986) *Proc. Natl. Acad. Sci. USA*, **83**, 9443–9447.
Wagner, G. (1993) *Curr. Opin. Struct. Biol.*, **3**, 748–754.
Wendoloski, J.J., Matthew, J.B., Weber, P.C. and Salemme, F.R. (1987) *Science*, **238**, 794–797.
Yang, D., Mittermaier, A., Mok, Y. and Kay, L.E. (1998) *J. Mol. Biol.*, **276**, 939–954.
Yang, D., Mok, Y., Muhandiram, D.R., Forman-Kay, J.D. and Kay, L.E. (1999) *J. Am. Chem. Soc.*, **121**, 3555–3556.
Yao, P., Xie, Y., Wang, Y.H., Sun, Y.L., Huang, Z.X., Xiao, G.T. and Wang, S.D. (1997) *Protein Eng.*, **10**, 575–581.